Received: 6 June 2022 | Accepted: 21 June 2022

DOI: 10.1002/lio2.853

ORIGINAL RESEARCH

Laryngoscope Investigative Otolaryngology

Augmentation and vocal fold biomechanics in a recurrent laryngeal nerve injury model

Solaleh Miar PhD[1,2] | Benjamin Walters MD[3] | Gabriela Gonzales MS[1,2] | Ronit Malka MD[3] | Amelia Baker MD[4] | Teja Guda PhD[1] | Gregory R. Dion MD[1,3,5]

[1]Department of Biomedical Engineering and Chemical Engineering, The University of Texas, San Antonio, Texas, USA

[2]USAF 59MDW/ST, Oak Ridge Institute for Science and Education, Oak Ridge, Tennessee, USA

[3]Department of Otolaryngology-Head and Neck Surgery, Brooke Army Medical Center, JBSA Fort Sam Houston, Texas, USA

[4]Department of Anesthesiology, Brooke Army Medical Center, JBSA Fort Sam Houston, Texas, USA

[5]Dental and Craniofacial Trauma Research Department, U.S. Army Institute of Surgical Research, Houston, Texas, USA

Correspondence
Gregory R. Dion, Dental and Craniofacial Trauma Research Department, U.S. Army Institute of Surgical Research, 3698 Chambers Pass, Bldg 3611, JBSA Fort Sam Houston, Texas, USA.
Email: gregrdion@gmail.com

Funding information
U.S. Air Force 59th Medical Wing, Grant/Award Number: Graduate Medical Education Fund

Abstract

Objectives/hypothesis: Composite vocal fold (VF) biomechanical data are lacking for augmentation after recurrent laryngeal nerve (RLN) injury. We hypothesize resulting atrophy decreases VF stiffness and augmentation restores native VF biomechanics.

Methods: Sixteen Yorkshire Crossbreed swine underwent left RLN transection and were observed or underwent carboxymethylcellulose (CMC) or calcium hydroxyapatite (CaHa) augmentation at 2 weeks. Biomechanical measurements (structural stiffness, displacement, and maximum load) were measured at 4 or 12 weeks. Thyroarytenoid (TA) muscle cross-sectional area was quantified and compared with two-way ANOVA with Tukey's post hoc test.

Results: After 4 weeks, right greater than left structural stiffness (mean ± SE) was observed (49.6 ± 0.003 vs. 28.4 ± 0.002 mN/mm), left greater than right displacement at 6.3 mN (0.54 ± 0.01 vs. 0.46 ± 0.01 mm, $p < .01$) was identified, and right greater than left maximum load (72.3 ± 0.005 vs. 40.8 ± 0.003 mN) was recorded. TA muscle atrophy in the injured group without augmentations was significant compared to the noninjured side, and muscle atrophy was seen at overall muscle area and individual muscle bundles. CMC augmentation appears to maintain TA muscle structure in the first 4 weeks with atrophy present at 12 weeks.

Conclusions: VF biomechanical properties match TA muscle atrophy in this model, and both CMC and CaHa injection demonstrated improved biomechanical properties and slower TA atrophy compared to the uninjured side. Taken together, these data provide a quantifiable biomechanical basis for early injection laryngoplasty to improve dysphonia and potentially improve healing in reversible unilateral vocal fold atrophy.

Level of evidence: N/A

KEYWORDS
augmentation, biomechanics, muscle atrophy, recurrent laryngeal nerve injury, swine

This manuscript was submitted for presentation at the American Laryngological Association Annual Meeting at the Combined Otolaryngology Spring Meetings in Dallas, TX, April 28-30, 2022.

This is an open access article under the terms of the Creative Commons Attribution-NonCommercial-NoDerivs License, which permits use and distribution in any medium, provided the original work is properly cited, the use is non-commercial and no modifications or adaptations are made.
© 2022 The Authors. *Laryngoscope Investigative Otolaryngology* published by Wiley Periodicals LLC on behalf of The Triological Society. This article has been contributed to by U.S. Government employees and their work is in the public domain in the USA.

1 | INTRODUCTION

Vocal fold paralysis, paresis, and atrophy are commonly treated with vocal fold augmentation, or injection laryngoplasty, to improve vocal function, breathing, and airway protection.[1,2] Providing bulk to the affected vocal fold(s) increases vocal fold contact area, improving control of glottic closure and mucosal wave generation with little to no recovery time required. Particularly in the setting of injury with potential for nerve recovery, resorbable materials such as carboxymethylcellulose (CMC), hyaluronic acid (HA), and calcium hydroxyapatite (CaHa) are common injectates in vocal fold augmentation.[3,4] However, these injectable materials vary in viscoelastic properties and resorption rates, complicating their effect on vocal fold biomechanics.[5] Improved understanding of laryngeal biomechanics after injection laryngoplasty may guide appropriate therapeutic intervention and optimize our current management of dysphonia.

Vocal fold atrophy after denervation has been examined in a variety of animal models and documented in the aging human larynx.[6–12] While degree of atrophy and involved musculature may vary based upon mechanism, chronicity, and location of injury, a causative relationship between atrophy and voice production remains unstudied. Furthermore, the thyroarytenoid (TA) muscle appears to maintain normal contractile force in chronic vocal fold immobility, suggesting multifactorial etiology of dysphonia in vocal fold atrophy and paresis.[13] Additionally, data regarding the effects of therapeutic intervention on vocal fold atrophy or paresis have been limited. Injection laryngoplasty with HA has been shown to promote viscoelastic properties closer to native vocal fold, but these studies have been sparse and limited HA used in rodent models.[14–16] To date, no studies examining CMC and CaHa, two of the most common materials used in vocal fold augmentation, have been published. Similarly, while some recent studies have examined the effect of stem cell or gene therapy on slowing vocal fold atrophy or promoting laryngeal muscle regeneration, these studies have been sparse and limited to animal models to date.[17–19]

Current studies on effects of recurrent laryngeal nerve (RLN) injury have been largely limited to morphologic assessments and electromyographic measurements of laryngeal musculature.[20–26] Biomechanical properties of vocal folds, particularly vocal fold stiffness, have been well described governing generation of symmetric and periodic mucosal waves, and thus regulating voice production.[27–31] However, unique laryngeal geometry poses challenges for the application of traditional mechanical measurement techniques, as most instruments are too large or require minimal geometric variations in the area of interest. To overcome this, various mechanical testing techniques have been adapted to measure vocal fold biomechanical properties.[27,28] Histologic and microcomputed tomography (microCT) scans have been utilized to correlate vocal fold biomechanical property variations with soft tissue morphologic differences, but lack the granularity needed for sub-millimeter analysis of vocal fold layers. Computational models of the larynx have provided insight into laryngeal fluid dynamics and biomechanical properties, but have limited clinical predictive ability.[32–36] Largely due to these limitations, no data to date exists regarding the natural history of progressive vocal fold muscle atrophy after RLN injury and resulting changes in laryngeal biomechanics.

In order to improve the reliability of composite vocal fold biomechanical property assessment, we previously described a novel technique to measure tissue biomechanics in the intact hemilarynx that permits for the assessment of the intact composite vocal fold structure to incorporate interactions of the vocal folds, lamina propria, and epithelium.[37,38] By taking advantage of unique microindentation techniques, as well as nanodynamic mechanical analysis, we demonstrated the ability to overcome these geometric challenges and collect meaningful data.[37,38] Our improved vocal fold biomechanical property measurement resolution also allowed for measurement of biomechanical changes during vocal fold wound healing.

As no current data exist on biomechanical composite vocal fold tissue properties after vocal fold injection augmentation, we designed a study to[1] quantify intact vocal fold biomechanical structural property differences after RLN injury and[2] quantify vocal fold biomechanical differences between CMC and CaHa after injection augmentation for RLN injury. We hypothesized that vocal fold biomechanical properties would vary from native vocal folds after RLN injury with progressive ipsilateral muscle atrophy and potential contralateral hypertrophy resulting in decreased stiffness, decreased elasticity, and increased displacement at a set force. Additionally, we hypothesized that CMC and CaHa would variably approximate native vocal fold biomechanical properties in RLN injuries and that these properties would change with time. For the current study, we quantified vocal fold structural stiffness, displacement at a set force, and TA muscle diameter over time after nerve transection and with augmentation with CMC or CaHa.

2 | MATERIALS AND METHODS

2.1 | Overview

After approval from the U.S. Air Force 59th Medical Wing Institutional Animal Care and Use Committee (protocol FWH20190101AR), 16 Yorkshire crossbreed swine (Sus scrofa) underwent left RLN transection, as the left side is most commonly injured from surgical management of neck and spine pathology.[39–43] Study groups were RLN transection alone, RLN transection with CMC injection, and RLN transection with CaHa injection. Animals were sacrificed at either 4 weeks postoperatively to assess for early post-injection results, clinically correlating with optimized post-procedural voice, or 12 weeks postoperatively to assess for waning post-injection results, clinically correlating with early return of dysphonia. All laryngeal specimens were harvested and underwent biomechanical and histological assessment of bilateral vocal folds.

2.2 | RLN transection

Swine were anesthetized via intramuscular injection of Telazol® or Telazol (4.4 mg/kg IM and Ketamine 2.2 mg/kg IM) and maintained using isoflurane as needed for anesthesia with vital signs monitored. Analgesia included Buprenorphine 0.01–0.05 mg/kg IM. Swine were placed supine and the anterior cervical area was prepped with

povidone-iodine solution after the area was pre-shaved. After the incision site was injected with 2 cc of 1% with 1:100,000 lidocaine/epinephrine and under sterile dissection, the left RLN was identified near the cricothyroid joint and a 2 cm portion of the nerve was excised to prevent any potential reanastamosis.

2.3 | Direct laryngoscopy and vocal fold augmentation

After 14 days and anesthesia via intramuscular injection of Telazol (4.4 and Ketamine 2.2 mg/kg IM) and isoflurane maintenance, swine underwent direct laryngoscopy while spontaneously ventilating to confirm left vocal fold immobility. Swine in the CMC or CaHa groups then underwent left vocal fold injection augmentation as well. A zero-degree, 30 cm-long telescope (Karl Storz Co., Culver City, CA) coupled with a camera was passed through the laryngoscope to maximize visualization. Injection augmentation proceeded under direct visualization with injection of 0.5 cc of CMC (Prolaryn Gel™, Merz North America Inc., Raleigh, N.C. USA) or CaHa (Prolaryn Plus™, Merz North America Inc., Raleigh, N.C. USA) just lateral to the left vocal fold bringing the injured vocal fold just past midline.

2.4 | Euthanasia and harvest

Swine were euthanized at study end points using 100 mg/kg IV pentobarbital, and then the larynx was harvested and immediately sectioned in the sagittal plane taking care to preserve the anterior commissure intact as done in our earlier studies.[37,38] Specimens were then frozen at −80 F until further analyses.

2.5 | Biomechanical analysis

Prior to mechanical testing, samples were thawed, fixed to a Plaster of Paris mold, and submerged in phosphate buffered saline (PBS) to maintain moisture as previously described.[44] Each specimen was positioned beneath a camera to align a template with predetermined indentation points along the vocal fold and regions of interest (Figure 1A). A 5 mm spherical indenter with an indentation velocity of 2 mm/s and an amplitude of 1 mm was used on a Biomomentum Mach-1 v500css (Laval, Quebec, Canada) mechanical tester with a 1.5 N uniaxial load cell. The structural stiffness at an indentation depth of 1 mm and displacement at a set force of 6.3 mN was measured using our previously described vocal fold indentation method.[44] The maximum load (N), corresponding to the peak load of the data curve, was also assessed across samples.

2.6 | Histological analysis

To quantify the TA muscle atrophy and evaluate the impact of the injectable materials on surrounding tissue, cross sections were collected from the anterior, middle, and posterior vocal folds. Figure 2 illustrates the sample collection for histological evaluation after mechanical characterization. Briefly, samples were cut perpendicularly to the vocal fold to 5 mm (thickness) cross-section cuts using high-profile histology

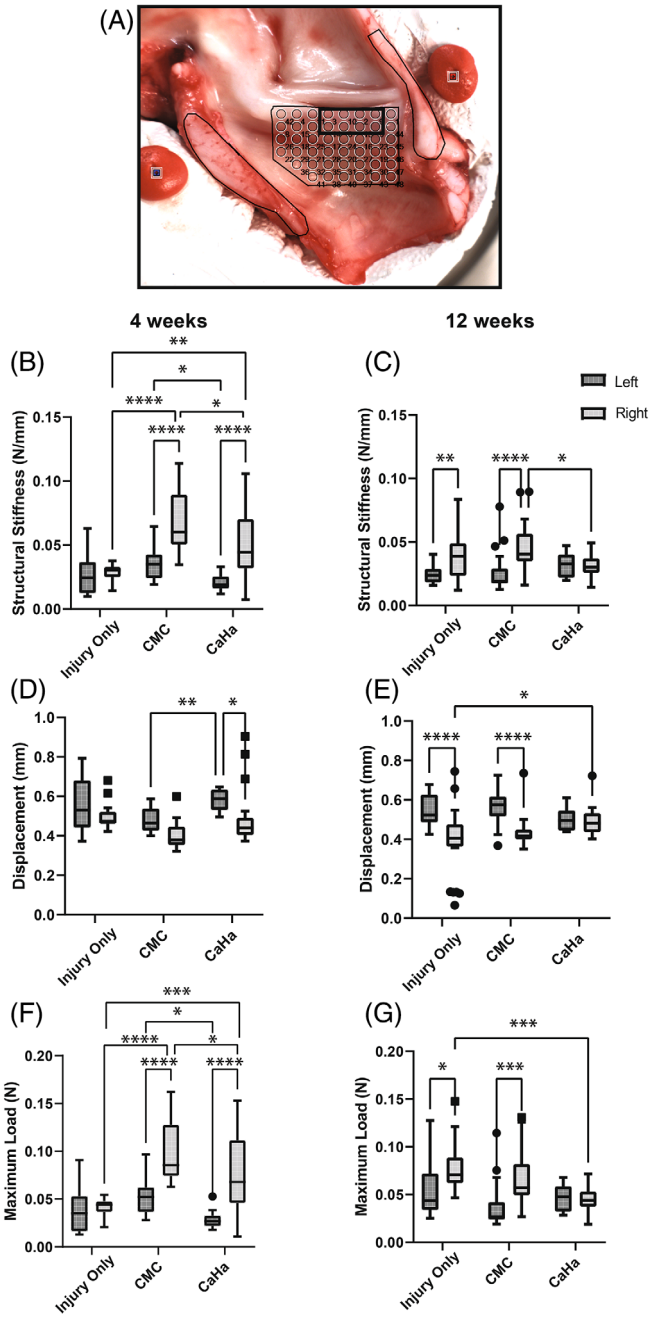

FIGURE 1 Evaluation of Mechanical Properties by indentation following laryngeal nerve injury and vocal fold augmentation. (A) Swine larynx specimen with indentation point mapping grid overlaid and inset indicates region selected for analysis along the midportion of the vocal fold. (B, C) Structural stiffness (N/mm), (D, E) displacement (mm), and (E, F) maximum load (N) were investigated after 4- and 12-weeks respectively for three groups after laryngeal nerve injury featuring augmentation with two composites (CMC, CaHa) and no treatment. Highlighted region includes indentation points of interest. (statistically significant differences are indicated by * < .05, ** < 0.01, *** < .001, **** < .0001)

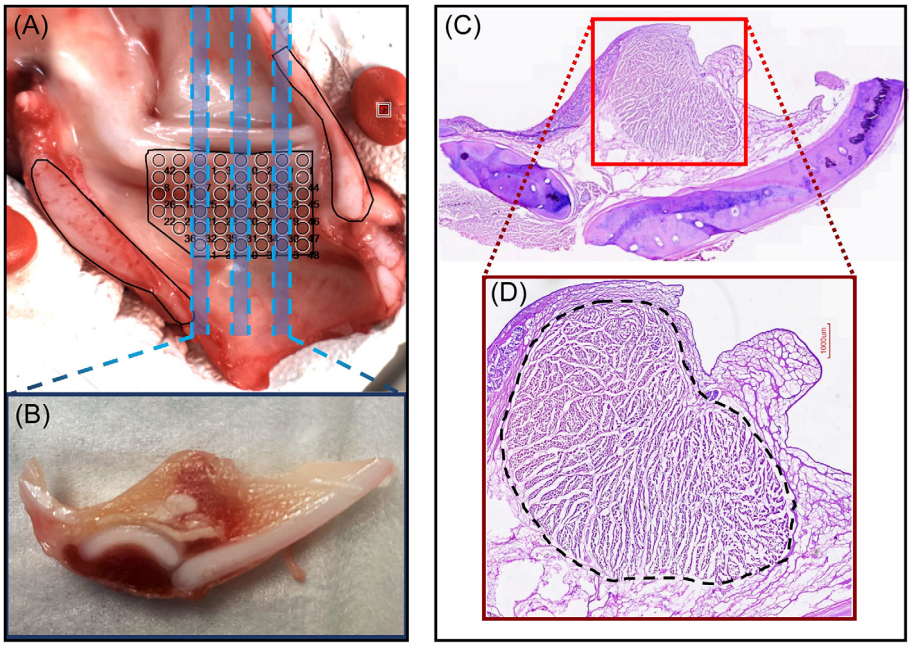

FIGURE 2 Histological methodology on the evaluation and quantification of the thyroarytenoid muscle. (A) 5 mm thick tissue sections collected from the back, middle, and front containing the vocal fold, subglottis, and supraglottis. (B) Tissue cross-section collected for histological evaluation before the fixation in formalin. (C) Tissue sample slide stained with H&E for histological evaluation and muscle area quantification. (D) Thyroarytenoid muscle area detected and marked in the histology image was successively quantified using ImageJ.

blades. Then, samples were fixed in 4% formalin solution and subsequently were mounted in disposable embedding molds filled with OCT compound. Molds containing the tissue cuts and OCT compound were stored at −80°C prior to sectioning. Frozen tissue segments were cut to a tissue thickness of 14 μm using a cryostat (Epredia™ NX70, Kalamazoo, MI) and thaw-mounted on glass slides. Slides were maintained at room temperature in the room temperature for 1 h to dry. To improve the adhesion of the tissue slices to the glass slides, slides were kept in chilled acetone at −20°C for 10 min. Subsequently, slides were hydrated with deionized water prior to staining. Samples were first stained with hematoxylin and eosin. Finally, stained tissue slides cuts were imaged with MoticEasyScan Pro 6 Slide Scanner (Motic Instruments, Schertz, TX) at 20× and 40×. TA muscle cross sectional areas were quantified using ImageJ software (v1.8.0, NIH Image, Bethesda, MD) (Figure 2D).

2.7 | Statistical analyses

The structural stiffness at the desired depth of 1 mm was determined by dividing the normal force at 1 mm by the indentation amplitude (1 mm). The displacement necessary to reach a normal force of 6.3 mN and maximum load were determined from the normal force versus normal position curves. The load 6.3 mN was selected because it was the smallest maximum load recorded across all specimens. Given the varying laryngeal dimensions across samples, indentation points were subdivided into zones corresponding to the anatomic regions of the vocal fold (free margin anterior, mid, or posterior, and distance towards the subglottis). Data collected from each indentation point within their respective zone were categorized based on their treatment group (no treatment, CMC, CaHa) and study endpoint (4 weeks, 12 weeks). Two-way analysis of variance (ANOVA) followed by Tukey's multiple comparisons testing was conducted with GraphPad Prism (v9.3.1 for Windows, San Diego, California).

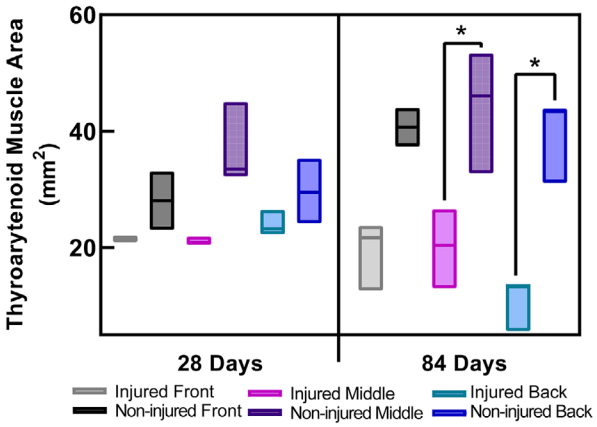

FIGURE 3 Thyroarytenoid muscle area in injured and noninjured sides. (A) The muscle area in the back, middle and front parts of the vocal cord in the injured and noninjured side for each animal is measured after 4 and 12 weeks to demonstrate the impact of nerve injury on different regions of the vocal cord. Statistically significant differences are indicated by $^*p < .05$. (B) Histological evaluation of thyroarytenoid muscle-only as an indication of the muscle atrophy after 12 weeks. This image is representative of the middle section of this muscle with and without the injury as the injured side shows a significantly different muscle area compared to the noninjured side.

3 | RESULTS

3.1 | Structural stiffness

Following 4 weeks, the structural stiffness (mean ± SE) on the right (49.6 ± 0.003 mN/mm) was significantly greater than the left (28.4 ± 0.002 mN/mm, $p < .0001$) across groups (Figure 1B). On the left side, augmentation with CMC (36.5 ± 0.003 mN/mm) presented a structural stiffness larger than with CaHa (20.5 ± 0.001 mN/mm) at

this time ($p = .02$). On the right, CMC augmentation produced a structural stiffness greater than both CaHa and no treatment ($p = .014$). Assessment at 12 weeks identified that right sided structural stiffness (38.7 mN/mm ± 0.002) remained greater than left (27.2 mN/mm ± 0.001) (Figure 1C). For the no treatment and CMC augmentation groups, right structural stiffness was greater ($p < .01$). Right vocal fold structural stiffness after left sided CMC augmentation was higher compared to the right vocal fold in the left sided CaHa injection group ($p = .024$).

3.2 | Displacement

The displacement (mean ± SE) at 6.3 mN for the left (0.54 ± 0.01 mm) was greater than the right (0.46 ± 0.01 mm) after 4 weeks ($p < 0.01$) across all treatment groups (Figure 1D). There was greater displacement in specimens (left side) with CaHa (0.58 ± 0.01 mm) augmentation than CMC (0.48 ± 0.01 mm) at this time ($p < 0.01$). After 12 weeks, the displacement at the set force remained similar in the left (0.54 ± 0.01 mm) and decreased in the right (0.44 ± 0.01 mm)

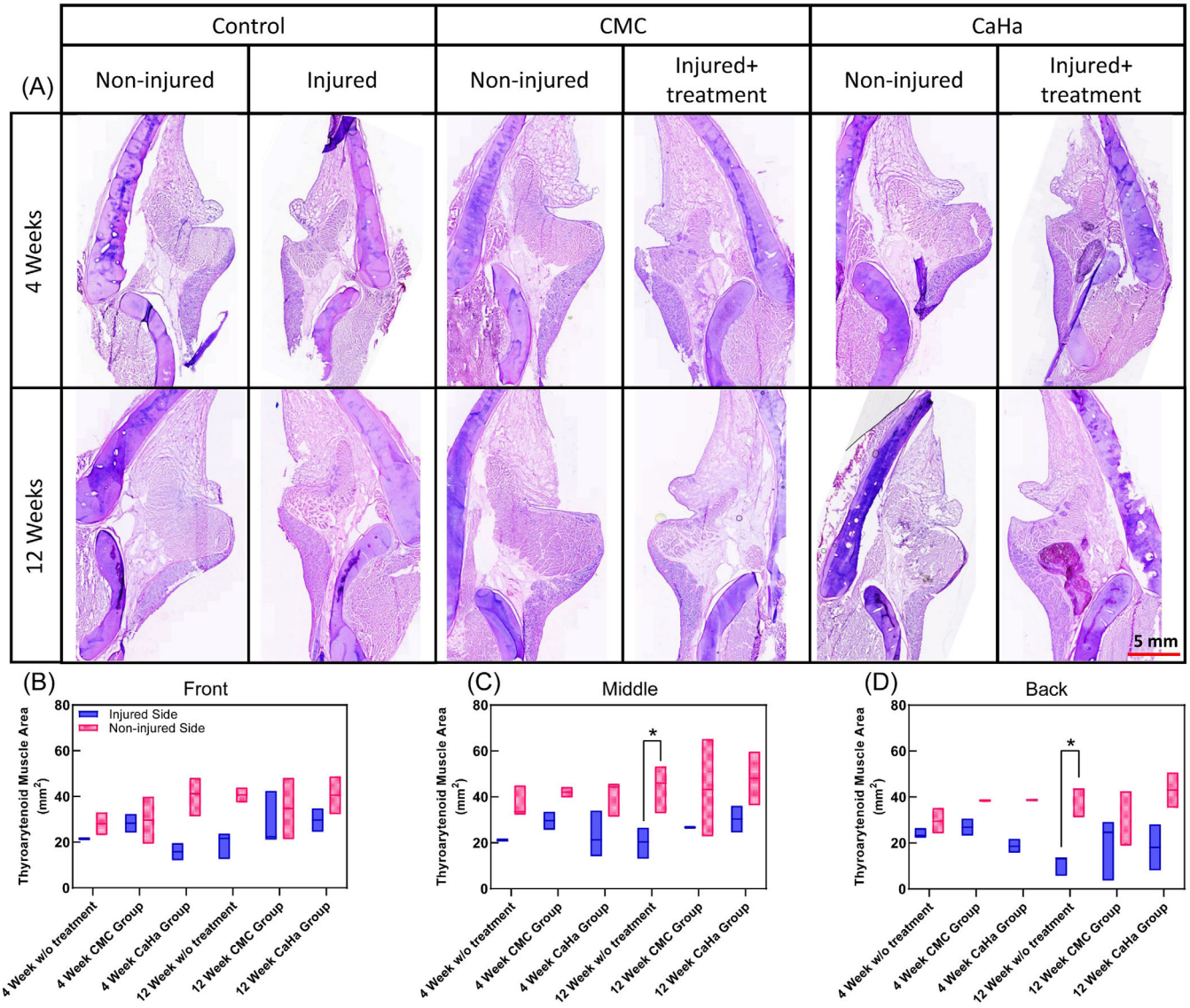

FIGURE 4 Histological evaluation of vocal cord in injured and noninjured groups and the impact of treatments on the morphological characteristics and measurements of the thyroarytenoid muscle. (A) H&E-stained cross-section of the vocal cord in the injured and noninjured models with and without augmentations with CMC and CaHa after 4 and 12 weeks. Images are presented at the magnification of 20×, and the scale bar presents 5 mm. Each group presents two paired images from the right (noninjured) and left (injured) sides of the animal to correlate the impact of muscle atrophy on the structure of the vocal cord. (B) Thyroarytenoid muscle area measurements in the front region of the vocal cord in noninjured and injured groups with no treatment, CMC augmentation, and CaHa augmentation after 4 and 12 weeks. (C) Thyroarytenoid muscle area measurements in the middle region of the vocal cord in noninjured and injured groups with no treatment, CMC augmentation, and CaHa augmentation after 4 and 12 weeks. (D) Thyroarytenoid muscle area measurements in the back region of the vocal cord in noninjured and injured groups with no treatment, CMC augmentation, and CaHa augmentation after 4 and 12 weeks. Statistically significant differences are indicated by $^*p < .05$

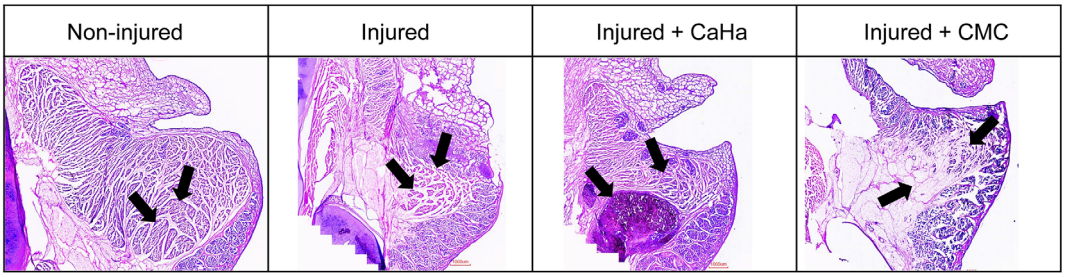

FIGURE 5 Histological evaluation of muscle bundles in thyroarytenoid muscle. Micrographs present the high-magnification images of the region of interest in the vocal fold and the dissociation of muscle bundle in injured groups with and without augmentation (CaHa or CMC) compared to a noninjured group after 12 weeks

(Figure 1E). For the groups with no treatment as well as when CMC augmentation was performed, the displacement observed was significantly greater for the treated side compared to the contralateral control after 12 weeks ($p < .001$). CaHa augmentation displayed higher displacement compared to the no treatment group for the right side of the specimen ($p = 0.019$).

3.3 | Maximum load

The maximum load (mean ± SE) was greater in the right (72.3 ± 0.005 mN) in comparison to the left (40.8 ± 0.003 mN) after 4 weeks (Figure 1F). The specimens (left side) treated with CMC withstood a greater maximum load (53.7 ± 0.005 mN) in comparison to those with CaHa (28.1 ± 0.002 mN) at this time ($p = .016$). Across treatment groups, CMC showed the greatest outcome for maximum load ($p = .022$). The load decreased for the right (61.9 ± 0.003 mN) and increased for the left (46.0 ± 0.003 mN) when evaluated at 12 weeks (Figure 1G). The CMC augmented and no treatment groups presented higher maximum load values than the injured left side ($p < .01$).

3.4 | Impact of nerve transection on TA muscle area

TA muscle areas of different vocal fold regions (front, middle, and back) on the injured side had atrophy throughout all regions at 4 and 12 weeks in swine with unilateral RLN injury without augmentation (Figure 3). Muscle atrophy was greater at 12 weeks than 4 weeks compared to the noninjured side in all regions. Not only did TA muscle area decrease on the RLN transection side, but TA individual muscle bundles revealed a distinct shrinkage with broad gaps between adjacent muscle bundles (Figure 4A and Figure 5).

3.5 | Impact of augmentation on the muscle area after nerve transection

CMC augmentation appears to maintain TA muscle structure in the first 4 weeks; however, atrophy is present at 12 weeks (Figure 4). CaHa augmentation also demonstrated overall preserved muscle structure after 4 and 12 weeks (Figure 4). As illustrated in Figure 4B–D, injured sides had decreased TA muscle area with or without augmentations. Only TA muscle atrophy in the injured group without augmentations was significant compared to the noninjured side in the middle ($p = .032$) and back (.041) regions after 12 weeks. Among all groups, the lowest muscle area occurred in the injured group at 12 weeks. Higher magnification images (40×) reveal the damage the nerve transection caused with smaller muscle bundles and TA muscle tissue loss (Figure 5). Although the CMC injection group demonstrated a compact muscle structure with smaller intrabundle muscle gaps, individual muscle bundle size is comparable to the other injured groups.

4 | DISCUSSION

Symmetric biomechanical properties across bilateral vocal folds is necessary for generation of symmetric, periodic mucosal waves during phonation.[27–31] With continued focus on novel augmentation materials, few models exist to quantify composite biomechanical vocal fold properties after augmentation in a RLN transection model that replicates clinical physiology. This model allowed for quantification of composite vocal fold biomechanics in conjunction with TA muscle atrophy after RLN transection with or without augmentation with the commonly injected CMC and CaHa materials. Furthermore, comparison of these biomechanical properties to uninjured contralateral vocal fold was performed, allowing assessment of how well injection laryngoplasty fares in achieving symmetric biomechanical properties to native tissue.

Control specimens without augmentation demonstrated significant reduction in stiffness and maximum load capability, and increase in displacement with standardized force application, compared to native tissue. However, injection augmentation with either CMC or CaHa induced vocal fold stiffening more closely approximating native tissue. This is presumed to not only allow for mucosal wave generation via fold medialization, but allow for more symmetric mucosal wave formation due to more closely-matching vocal fold biomechanical properties. Notably, while CMC and CaHa have similar baseline mechanical properties, vocal folds injected with CMC demonstrated biomechanical properties that more closely matched uninjured vocal fold tissue. This suggests the impact of injection laryngoplasty is not

just due to biomechanical properties of the injectate but also local tissue reaction, most likely a local inflammatory response that increases tissue stiffness throughout the vocal cord. Unilateral atrophy additionally appeared to minimally alter biomechanical properties of the unaffected contralateral side; while this mechanism remains unclear, it may be due to complex laryngeal innervation patterns, which often include small bilateral innervation components, or may be secondary to broader inflammatory effects in response to denervation.

Cross-sectional area of TA muscles, used to evaluate degree of vocal fold muscle atrophy, indicated that, although the CMC may maintain the overall structure in the four-week group, muscle atrophy developed in all groups by the 12 week point. However, CaHa augmentation demonstrated reduced atrophy compared to CMC, which is hypothesized to be secondary to longer time to degradation of CaHa compared to CMC. These findings support the impact of using early augmentation techniques to reduce early muscle atrophy in unilateral vocal fold injury, This additionally provides further clinical rationale for early augmentation in potentially reversible nerve injury within the first year after injury beyond improvement of dysphonia and aspiration symptoms, as reducing early atrophy in reversible injury would be expected to hasten recovery and return to baseline function.

Several limitations of the current study warrant discussion. Four of 96 histologic sections (4% of specimens) failed to produce adequate muscle visualization for area measurement second to local tissue damage during processing and sectioning that precluded adequate area measurement; however, other regions (front, middle, back) of each specimen were available such that muscle analysis was performed on each hemi-larynx. Another limitation originates with the muscle area quantification. In this assessment, overall muscle cross-sectional area was compared between the RLN transection side and the uninjured side. In many cases, the overall area over-represents the TA size in the RLN injury side, as the actual muscle bundles themselves are smaller. These findings could strengthen differences identified on overall TA muscle cross-sectional area.

Additionally, biomechanical test parameters may impact analyses. Displacement was measured at 6.3 mN, as this was the smallest maximal load identified across all specimens, ensuring that each specimen would have comparable values. It is possible that additional differences between groups may occur with lower set forces. Similarly, 1 mm depth was selected for normal force and structural stiffness, as along the free edge of the true vocal fold this should reflect composite epithelium/muscle properties. Alternative depth selections could result in varied composite tissue properties. Additional study endpoints could provide further information on timing of when atrophy is first seen (earlier timepoints) or if additional atrophy may occur (later timepoints). Finally, it should be noted that biomechanical testing required a cycle of freezing tissues and subsequently thawing them for analysis. While repeated freeze–thaw cycles have been shown to increase storage, loss, and complex modulus in testing, initial data surrounding development of the microindentation technique utilized was obtained with all tissues undergoing a single freeze–thaw cycle.[38] Tissue handling in this study was consistent with this prior technique validation, and was additionally internally consistent among the groups tested in this study. Furthermore, it should be emphasized that clinical utility of biomechanical properties of vocal fold tissue are most valuable in comparison to similarly-processed controls rather than in analysis of absolute storage modulus values.

5 | CONCLUSION

VF biomechanical properties match TA muscle atrophy in this RLN transection model, with increased displacement and lower structural stiffness and smaller muscle areas on the injured side. While both CMC and CaHa injection demonstrated improved biomechanical properties and slower TA atrophy compared to the uninjured side, this effect diminishes with time. Furthermore, while CaHa degrades at a much slower rate, CMC injection appears to achieve vocal fold biomechanical properties closest to native vocal fold tissue and have these properties persist longer than CaHa. Taken together, these data provide a quantifiable biomechanical basis for early injection laryngoplasty to both improve dysphonia and potentially improve healing in reversible unilateral vocal fold atrophy.

CONFLICTS OF INTEREST

The authors have no conflicts of interest or financial disclosures.

ORCID

Ronit Malka https://orcid.org/0000-0002-9864-2698
Teja Guda https://orcid.org/0000-0002-3218-2916
Gregory R. Dion https://orcid.org/0000-0003-4389-3104

REFERENCES

1. Dion GR, Fritz MA, Teng SE, et al. Impact of vocal fold augmentation and laryngoplasty on dyspnea in patients with glottal incompetence. *Laryngoscope*. 2018;128(2):427-429. doi:10.1002/lary.26850
2. Dion GR, Achlatis E, Teng S, et al. Changes in peak airflow measurement during maximal cough after vocal fold augmentation in patients with glottic insufficiency. *JAMA Otolaryngol Head Neck Surg*. 2017;143(11):1141-1145. doi:10.1001/jamaoto.2017.0976
3. King JM, Simpson CB. Modern injection augmentation for glottic insufficiency. *Curr Opin Otolaryngol Head Neck Surg*. 2007;15(3):153-158. doi:10.1097/MOO.0b013e3281084e61
4. Sulica L, Rosen CA, Postma GN, et al. Current practice in injection augmentation of the vocal folds: indications, treatment principles, techniques, and complications. *Laryngoscope*. 2010;120(2):319-325. doi:10.1002/lary.20737
5. Kwon TK, Buckmire R. Injection laryngoplasty for management of unilateral vocal fold paralysis. *Curr Opin Otolaryngol Head Neck Surg*. 2004;12(6):538-542.
6. Woodson GE, Hughes LF, Helfert R. Quantitative assessment of laryngeal muscle morphology after recurrent laryngeal nerve injury: right vs. left differences. *Laryngoscope*. 2008;118(10):1768-1770. doi:10.1097/MLG.0b013e31817f1940
7. Shindo ML, Herzon GD, Hanson DG, Cain DJ, Sahgal V. Effects of denervation on laryngeal muscles: a canine model. *Laryngoscope*. 1992;102(6):663-669. doi:10.1288/00005537-199206000-00012
8. Sahgal V, Hast MH. Effect of denervation on primate laryngeal muscles: a morphologic and morphometric study. *J Laryngol Otol*. 1986;100(5):553-560.

9. Kirchner JA. Atrophy of laryngeal muscles in vagal paralysis. *Laryngoscope*. 1966;76:1753-1765. doi:10.1288/00005537-196611000-00001
10. Wang H, Li X, Xu W. Characteristics of early internal laryngeal muscle atrophy after recurrent laryngeal nerve injuries in rats. *Laryngoscope*. 2021;131(4):E1256-e1264. doi:10.1002/lary.29210
11. Steele BN, Wan J, Ku JP, Hughes TJ, Taylor CA. In vivo validation of a one-dimensional finite-element method for predicting blood flow in cardiovascular bypass grafts. *IEEE Trans Biomed Eng*. 2003;50(6):649-656. doi:10.1109/TBME.2003.812201
12. Martins RH, Benito Pessin AB, Nassib DJ, Branco A, Rodrigues SA, Matheus SM. Aging voice and the laryngeal muscle atrophy. *Laryngoscope*. 2015;125:2518-2521. doi:10.1002/lary.25398
13. Johns MM, Urbanchek M, Chepeha DB, Kuzon WM Jr, Hogikyan ND. Thyroarytenoid muscle maintains normal contractile force in chronic vocal fold immobility. *Laryngoscope*. 2001;111:2152-2156. doi:10.1097/00005537-200112000-00014
14. Borzacchiello A, Mayol L, Garskog O, Dahlqvist A, Ambrosio L. Evaluation of injection augmentation treatment of hyaluronic acid based materials on rabbit vocal folds viscoelasticity. *J Mater Sci Mater Med*. 2005;16(6):553-557. doi:10.1007/s10856-005-0531-2
15. Dahlqvist A, Garskog O, Laurent C, Hertegard S, Ambrosio L, Borzacchiello A. Viscoelasticity of rabbit vocal folds after injection augmentation. *Laryngoscope*. 2004;114(1):138-142. doi:10.1097/00005537-200401000-00025
16. Choi JS, Kim NJ, Klemuk S, et al. Preservation of viscoelastic properties of rabbit vocal folds after implantation of hyaluronic acid-based biomaterials. *Otolaryngol Head Neck Surg*. 2012;147(3):515-521. doi:10.1177/0194599812446913
17. Dirja BT, Yoshie S, Ikeda M, et al. Potential of laryngeal muscle regeneration using induced pluripotent stem cell-derived skeletal muscle cells. *Acta Otolaryngol*. 2016;136(4):391-396. doi:10.3109/00016489.2015.1126351
18. Paniello RC, Brookes S, Bhatt NK, Bijangi-Vishehsaraei K, Zhang H, Halum S. Improved adductor function after canine recurrent laryngeal nerve injury and repair using muscle progenitor cells. *Laryngoscope*. 2018;128(7):E241-e246. doi:10.1002/lary.26992
19. Goto T, Ueha R, Sato T, Fujimaki Y, Nito T, Yamasoba T. Single, high-dose local injection of bFGF improves thyroarytenoid muscle atrophy after paralysis. *Laryngoscope*. 2020;130(1):159-165. doi:10.1002/lary.27887
20. Paniello RC, Rich JT, Debnath NL. Laryngeal adductor function in experimental models of recurrent laryngeal nerve injury. *Laryngoscope*. 2015;125(2):E67-E72. doi:10.1002/lary.24947
21. Toya Y, Kumai Y, Minoda R, Yumoto E. Modulation of nerve fibers in the rat thyroarytenoid muscle following recurrent laryngeal nerve injury. *Acta Otolaryngol*. 2012;132(3):305-313. doi:10.3109/00016489.2011.637176
22. Braund KG, Steiss JE, Marshall AE, Mehta JR, Amling KA. Morphologic and morphometric studies of the intrinsic laryngeal muscles in clinically normal adult dogs. *Am J Vet Res*. 1988;49:2105-2110.
23. Lee KE, Jee HG, Kim HY, Park WS, Park SH, Youn YK. Development of a canine model for recurrent laryngeal injury by harmonic scalpel. *Lab Anim Res*. 2012;28(4):223-228. doi:10.5625/lar.2012.28.4.223
24. Bjorck G, Margolin G, Maback GM, Persson JK, Mattsson P, Hydman J. New animal model for assessment of functional laryngeal motor innervation. *Ann Otol Rhinol Laryngol*. 2012;121:695-699. doi:10.1177/000348941212101013
25. Bhatt NK, Park AM, Al-Lozi M, Paniello RC. Compound motor action potential quantifies recurrent laryngeal nerve innervation in a canine model. *Ann Otol Rhinol Laryngol*. 2016;125(7):584-590. doi:10.1177/0003489416637386
26. Nishio N, Fujimoto Y, Suga K, et al. Autologous fat injection therapy including a high concentration of adipose-derived regenerative cells in a vocal fold paralysis model: animal pilot study. *J Laryngol Otol*. 2016;130:914-922. doi:10.1017/S0022215116008707
27. Dion GR, Jeswani S, Roof S, et al. Functional assessment of the ex vivo vocal folds through biomechanical testing: a review. *Mater Sci Eng C Mater Biol Appl*. 2016;64:444-453. doi:10.1016/j.msec.2016.04.018
28. Miri AK. Mechanical characterization of vocal fold tissue: a review study. *J Voice*. 2014;28(6):657-667. doi:10.1016/j.jvoice.2014.03.001
29. Hirano M. Morphological structure of the vocal cord as a vibrator and its variations. *Folia Phoniatr Logop*. 1974;26(2):89-94.
30. Hirano M. Vocal mechanisms in singing: laryngological and phoniatric aspects. *J Voice*. 1988;2(1):51-69.
31. Pickup BA, Thomson SL. Influence of asymmetric stiffness on the structural and aerodynamic response of synthetic vocal fold models. *J Biomech*. 2009;42(14):2219-2225.
32. Chang S, Tian FB, Luo H, Doyle JF, Rousseau B. The role of finite displacements in vocal fold modeling. *J Biomech Eng*. 2013;135:111008. doi:10.1115/1.4025330
33. Mylavarapu G, Mihaescu M, Fuchs L, Papatziamos G, Gutmark E. Planning human upper airway surgery using computational fluid dynamics. *J Biomech*. 2013;46(12):1979-1986. doi:10.1016/j.jbiomech.2013.06.016
34. Sidlof P, Zorner S, Huppe A. A hybrid approach to the computational aeroacoustics of human voice production. *Biomech Model Mechanobiol*. 2015;14(3):473-488. doi:10.1007/s10237-014-0617-1
35. Gokcan MK, Kurtulus DF, Ustuner E, et al. A computational study on the characteristics of airflow in bilateral abductor vocal fold immobility. *Laryngoscope*. 2010;120(9):1808-1818. doi:10.1002/lary.21003
36. Markow M, Janecki D, Orecka B, Misiolek M, Warmuzinski K. Computational fluid dynamics in the assessment of patients' postoperative status after glottis-widening surgery. *Adv Clin Exp Med*. 2017;26(6):947-952. doi:10.17219/acem/64235
37. Dion GR, Benedict PA, Coelho PG, Amin MR, Branski RC. Impact of medialization laryngoplasty on dynamic nanomechanical vocal fold structure properties. *Laryngoscope*. 2018;128(5):1163-1169. doi:10.1002/lary.26963
38. Dion GR, Coelho PG, Teng S, Janal MN, Amin MR, Branski RC. Dynamic nanomechanical analysis of the vocal fold structure in excised larynges. *Laryngoscope*. 2017;127(7):E225-e230. doi:10.1002/lary.26410
39. Weisberg NK, Spengler DM, Netterville JL. Stretch-induced nerve injury as a cause of paralysis secondary to the anterior cervical approach. *Otolaryngol Head Neck Surg*. 1997;116(3):317-326. doi:10.1016/S0194-59989770266-3
40. Beutler WJ, Sweeney CA, Connolly PJ. Recurrent laryngeal nerve injury with anterior cervical spine surgery risk with laterality of surgical approach. *Spine (Phila Pa 1976)*. 2001;26(12):1337-1342.
41. Netterville JL, Koriwchak MJ, Winkle M, Courey MS, Ossoff RH. Vocal fold paralysis following the anterior approach to the cervical spine. *Ann Otol Rhinol Laryngol*. 1996;105(2):85-91. doi:10.1177/000348949610500201
42. Alimoglu O, Akdag M, Kaya B, et al. Recurrent laryngeal nerve palsy after thyroid surgery. *Int Surg*. 2008;93(5):257-260.
43. Serpell JW, Lee JC, Yeung MJ, Grodski S, Johnson W, Bailey M. Differential recurrent laryngeal nerve palsy rates after thyroidectomy. *Surgery*. 2014;156(5):1157-1166. doi:10.1016/j.surg.2014.07.018
44. Dion GR, Lavoie JF, Coelho P, Amin MR, Branski RC. Automated indentation mapping of vocal fold structure and cover properties across species. *Laryngoscope*. 2019;129(1):E26-E31. doi:10.1002/lary.27341

How to cite this article: Miar S, Walters B, Gonzales G, et al. Augmentation and vocal fold biomechanics in a recurrent laryngeal nerve injury model. *Laryngoscope Investigative Otolaryngology*. 2022;7(4):1057-1064. doi:10.1002/lio2.853